	Experiments Division

ALBA Project Document No:	*EDMS Document No.*	*Created: 21/12/2007*	*Pages: 12*
EXD-BL22-QWP-0001		*Modified: 09/01/2008*	*Rev. No.: 2*

Conceptual Design Report

Requirements for quarter-wave plates on ALBA XAS beamline

Prepared by:	*Checked by:*	*Approved by:*
Konstantin Klementiev		

Distribution List

Contents

Overview

This document describes the x-ray polarizer to be installed at the ALBA XAS beamline. It features:

(i) large energy range 2.4–15 keV covered by two crystals;

(ii) a double crystal set to (a) choose between circular and vertical linear polarization and (b) to perform polarimetry using a crystal analyzer;

(iii) fast flip of helicity.

The document provides a basis for market survey of available crystals of optimal thickness, sizes and mosaicity.

1 Introduction

To realize x-ray magnetic circular dichroism (XMCD) experiments the usage of a quarter-wave plate (QWP) is considered to be a single way at a beamline with a wiggler source. A considerable advantage of such a polarizer is the possibility to rapidly flip the helicity and thus to have the dichroic spectra in a constantly directed magnetic field, enabling element-selective hysteretic magnetization studies.

With doubling the crystals set one gets a half-wave plate (HWP) polarizer which transforms the horizontal polarization to the vertical one. An interesting application for the vertically polarized beam could be angular (momentum transfer) dependent Raman studies with a fluorescence analyzer moving in horizontal plane [1].

This Report offers optimization procedure of the QWP crystals in respect to their size and orientation, and gives expected values of polarization rate at various mosaicity as parameter.

The properties of the monochromatic beam assumed in this CDR are described in [2].

2 Principles of quarter-wave plates

The x-ray polarization phenomena were reviewed in [3,4]. For the case of a strongly divergent beam (here, 590h×77v arcsec^2 which is to be compared with the Darwin widths at the lowest reachable energy, i.e. ~13 arcsec for Be(100) at 3.5 keV, ~21 arcsec for diamond(111) at 3.5 keV, ~51 arcsec for graphite(002) at 2.4 keV) the only feasible implementation of a crystal QWP is to adjust the crystal outside the domain of reflection where the birefringence is lower but still exists. In this mode, the phase shift induced by the phase plate is the same for the diffracted and the forward-diffracted beams and is given by:

$$\phi = -\frac{\pi}{2}\frac{\mathrm{Re}(\chi_h\chi_{\bar{h}})\sin(2\theta)}{\lambda\Delta\theta}t \equiv -\frac{\pi}{2}A\frac{t}{\Delta\theta}, \qquad (1)$$

where $\Delta\theta$, so called angular offset, is the difference between the angle of incidence and the incidence at the middle of the rocking curve, χ_h and $\chi_{\bar{h}}$ are the Fourier harmonic of the electric susceptibility for the reciprocal-lattice vectors h and $\bar{h}$, t is the beam path. Equation (1) is valid when the angular offset is much greater than the Darwin width. As follows from (1), it is possible to obtain from linear polarization either right- or left-handed circular polarization by going from positive to negative offsets. For a given crystal the efficiency is larger for stronger reflections.

A linearly polarized wave with polarization vector inclined by an angle ψ with respect to the plane of diffraction of a polarizer crystal acquires the circular polarization rate

$$\tau \equiv s_3 / s_0 = \sin(2\psi)\,\mathrm{Im}\left\langle e^{i\phi}\right\rangle, \qquad (2)$$

where $s_{0,3}$ are the Stokes parameters. τ maximizes at $\psi = \pi/4$ and $\phi = \pi/2$. Due to x-ray beam divergence and imperfection of the polarizer crystal the angular offset $\Delta\theta$ is variable over the beam cross-section, therefore ϕ deviates from $\pi/2$ and thus $\tau<1$. The variation of ϕ is relatively smaller at larger nominal angular offsets. However, in going to larger $\Delta\theta$ at a given energy and for a given crystal (given A value in equation (1)) t must be increased proportionally to $\Delta\theta$ and then the transmission $\exp(-\mu t)$ of the polarizer crystal is lower.

Finally, a high polarization rate can be obtained at the expense of intensity absorbed by the polarizer crystal. Because of the tradeoff between circular polarization rate and intensity losses, crystals of low absorption are preferred.

3 Preliminary considerations: requirements, starting conditions and materials selection

Energy range for the QWP should cover:

1) 2(2.4 reachable)–4 keV for the L edges of 4d elements from Y(Mo reachable) to Ag,
2) 4.9–10 keV for the K edges of 3d elements from Ti to Cu,
3) 5.4–15 keV for the L edges of 5d and 4f elements from La to Au,
4) 17–27 keV for the K edges of 4d elements from Y to Ag.

NB: As will be shown below, the latter range is hardly accessible with QWPs of reasonable size.

Beam properties at the ALBA XAS beamline:

Full beam angular size after the focusing mirror = 590h×77v arcsec2. Maximum beam size at the position of QWP (2.5 m upstream the sample position) = 8h×1.5v mm^2. XZ size (i.e. at 45º to x and z axes) is ~5.8 mm.

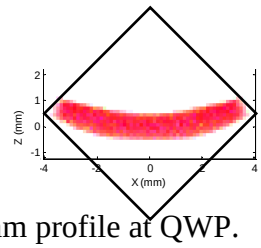

Fig. 1. Beam profile at QWP.

Taking into account the beam divergence, the lowest angular offset of the QWP at the ALBA XAS beamline should be higher than $\Delta\theta$ = 50 arcsec. Figure 2 shows the transmission of QWPs made of several light perfect crystals and also silicon as a common crystal. The effective thickness was calculated following equation (1) as $t = \Delta\theta/A$ using the code Xinpro1.2 / XOP2.1 [5]. Notice that the thickness here is not constant but different (and optimal) *at each energy*; these ideal curves can be obtained with a large number of crystals each having optimal thickness at a given energy. Even for the relatively low angular offset of 50 arcsec and correspondingly quite thin crystals, absorption by Si and NaCl is rather high. LiF crystals are difficult to handle and it is difficult to obtain crystals of good quality (low mosaicity). The only candidates as polarizer crystals are beryllium, diamond and graphite, the latter being the only one for the lowest energy. For these crystals the A value from equation (1) which can be called *linear helix density* and the linear absorption coefficient are shown in Figure 3.

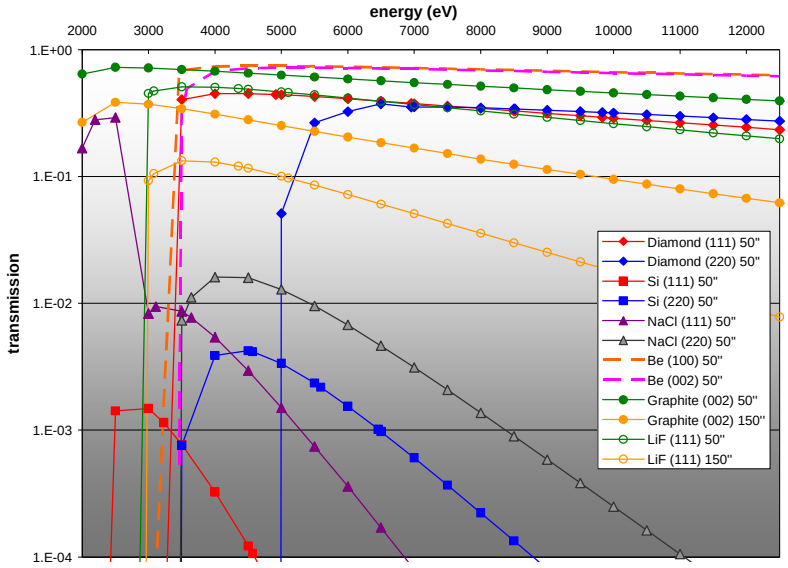

Figure 2. Transmission of QWPs made of silicon and several light *perfect* crystals.

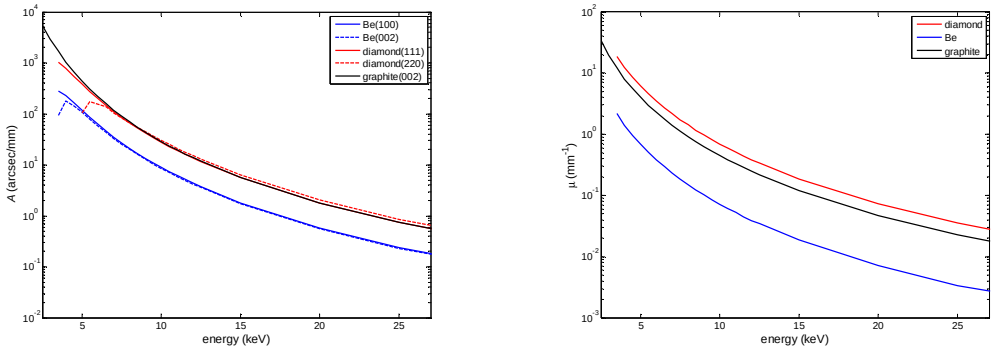

Figure 3. The QWP linear helix density *A* and absorption coefficient for the three crystals.

Finally, the three crystals: beryllium, diamond and graphite will be considered below as possible materials for QWPs.

4 Optimization criteria and strategy

The XMCD signal is proportional to the circular polarization rate τ. On the other hand, the signal-to-noise ratio for each of the measured components μ_R or μ_L in the XMCD signal $(\mu_R - \mu_L)/(\mu_R + \mu_L)$ is proportional to square root of incident intensity, either in transmission or fluorescence or total electron yield detection schemes [6]. Finally, the signal-to-noise ratio is

$$\frac{S}{N} \propto \tau (I_0 e^{-\mu t})^{1/2}, \qquad (3)$$

where the beam path $t = \Delta\theta_{\pi/2}/A$, is a function of independent variable $\Delta\theta_{\pi/2}$; intensity I_0 before the QWP and the polarization rate τ are calculated in ray tracing done with ED-Shadowrunner [7] which is a Matlab script running the Shadow ray tracing code [8,5]:

$$\tau = \sin(2\psi)\,\mathrm{Im}\left(\frac{1}{N_{rays}}\sum_{rays}\exp\left[i\frac{\pi}{2}\frac{\Delta\theta_{\pi/2}}{\Delta\theta_{\pi/2}+\delta_{ray}}\right]\right), \tag{4}$$

$$\delta_{ray} = x'_{ray}\cos\psi + z'_{ray}\sin\psi - \frac{E_{ray}-\overline{E}}{\overline{E}}\tan\theta_{QWP}\,. \tag{5}$$

The latter term in δ_{ray} accounts for energy distribution due to finite resolution of monochromator and is of less importance in comparison to the influence of beam divergence.

Notice that the QWP thickness is not constant here but optimal at each energy.

The maximization of signal-to-noise ratio at varying energy, angular offset, beam aperture and mosaicity was done for the five diffracting planes: Be (100), Be (002), diamond (111), diamond (220) and graphite (002). At this stage, the diffraction geometry (Laue or Bragg, symmetric or asymmetric) is not important; this becomes important when selecting the optimal crystal thickness in going from the optimal angular offset.

5 Optimization "aperture *vs.* angular offset" (perfect crystals)

Closing the beam aperture, on one hand, increases the polarization rate because of better beam collimation but on the other hand, this decreases the intensity. Here the S/N ratio is studied as a function of the three independent variables: *X* aperture, *Z* aperture (as fractional values from 0 to 1 relative the full beam opening) and angular offset.

The figures below show (i) contour plots of S/N ratio as filled colored areas, (ii) circular polarization rate as black contour lines and (iii) transmission of the polarizer crystal as white contour lines. The figures can be better viewed on screen with a high magnification.

***E*=3500 eV** Be(100) diamond (111) graphite (002)

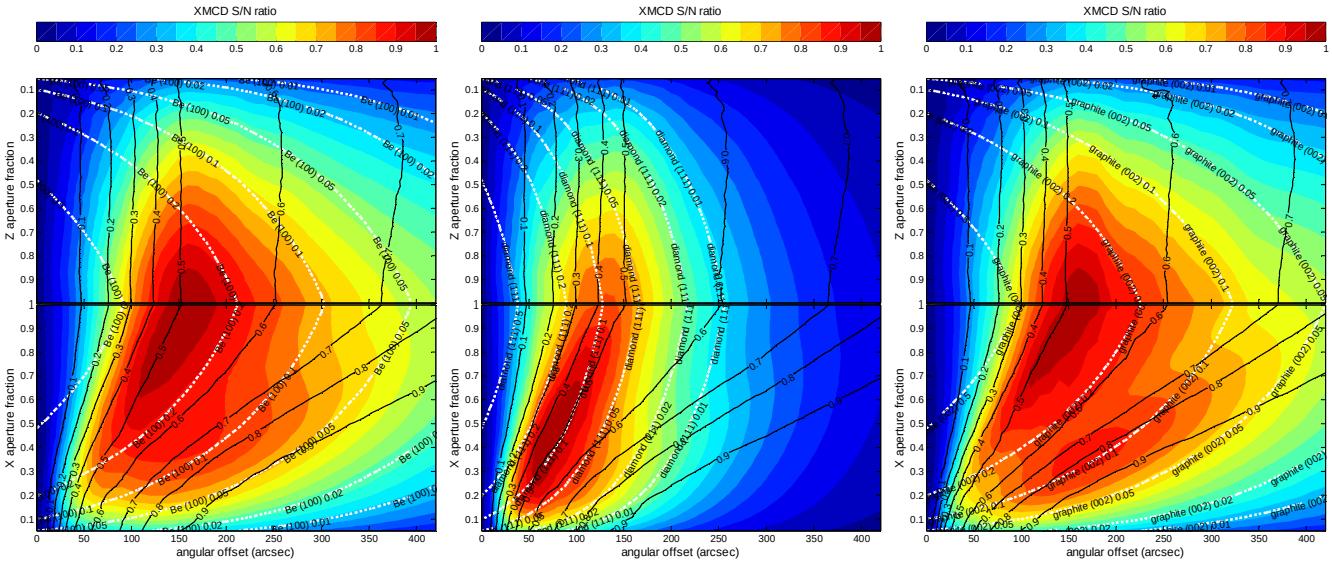

***E*=9000 eV** Be(100) diamond (111) graphite (002)

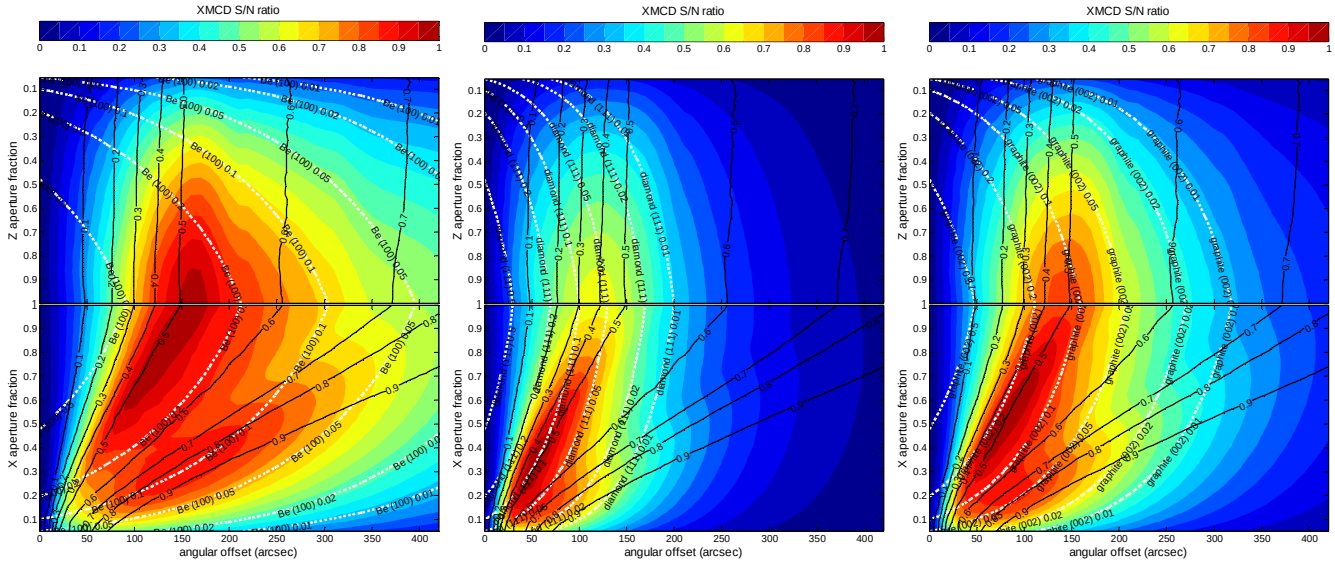

***E*=25000 eV** Be(100) diamond (111) graphite (002)

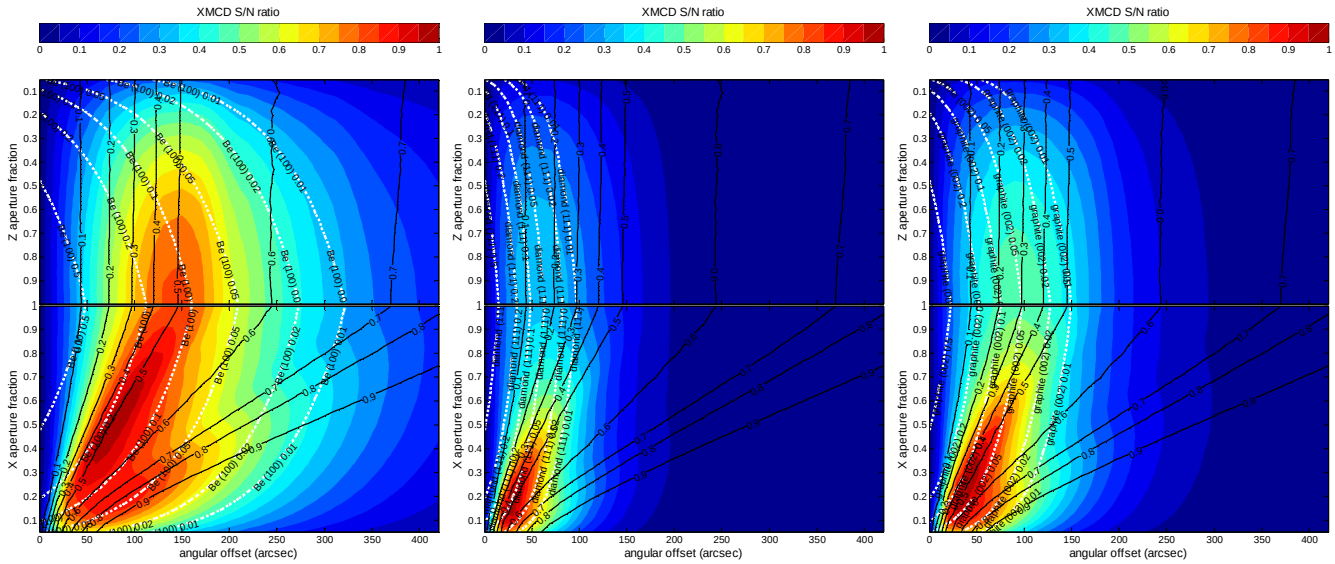

Observations:

Because the divergence *X*' is much higher than *Z*', closing the *Z* aperture does not improve the S/N ratio. The optimal aperture decreases for higher energies. At the optimum condition for the S/N ratio, the polarization rate in all cases is ~0.5.

Summary:

X aperture should be closed depending on energy and the polarizer crystal type.

6 Influence of mosaicity

The mosaic spread adds directly to δ_{ray} in Equation (5). In this exercise the mosaicity spread is assumed to have normal distribution with FWHM specified below by word "mosaicity".

The plots of S/N ratio in "*X* aperture *vs.* angular offset" coordinates are repeated here from the previous section (zero mosaicity) and compared with the cases of "good" mosaicity: 80 arcsec for Be and diamond crystals and 150 arcsec for graphite crystal.

***E*=3500 eV** Be(100) diamond (111) graphite (002)

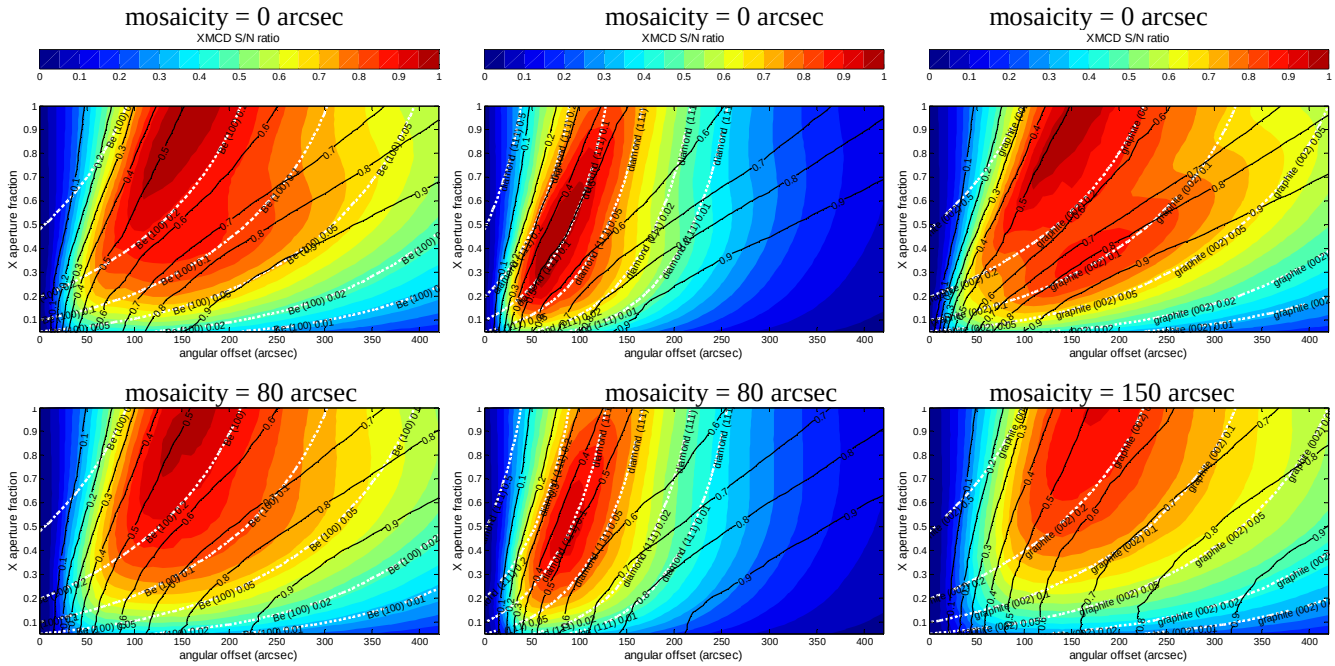

Observations:

Mosaicity spread deteriorates the polarization rate. With a reasonable mosaicity spread the optimal aperture remains almost unaffected and the optimal angular offset slightly increases at the expense of intensity.

Summary:

The optimization should be repeated for the mosaicity values of the real crystals bought for the polarizer. All the following results assume the "good" mosaicity values specified above.

7 Optimal aperture and optimal angular offset

The optimal *X* apertures and angular offsets are summarized below for the whole energy range. The S/N ratio is normalized to 1 *at each energy independently*.

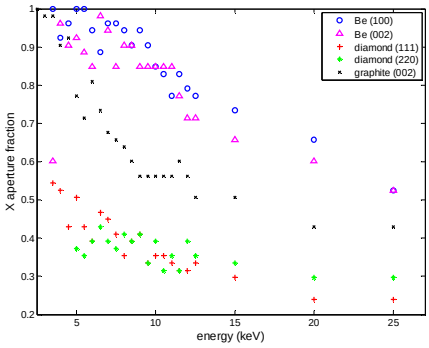

Be(100) Be(002) diamond (111) diamond (220) graphite (002)

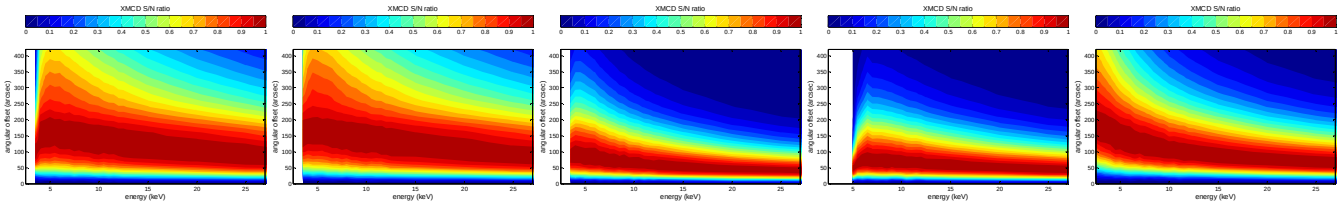

8 Size of QWPs

The above graphs are the base for finding the optimal crystal thickness and the optimal diffraction geometry.

The crystals plates are assumed to be Be (100), diamond (111) and graphite (001). The following diffraction geometries are then possible: Be 100 symmetric Bragg, Be 010 asymmetric Laue with $\alpha = \pm 60^{\circ}$, Be 002 symmetric Laue, diamond 111 symmetric Bragg, diamond 11–1 asymmetric Laue with $\alpha = \pm 70.5^{\circ}$, diamond 2–20 symmetric Laue, diamond 220 asymmetric Laue with $\alpha = \pm 35.3^{\circ}$ and graphite 002 symmetric Bragg.

The best geometry is the one which (i) works at the most wide energy range (most flat 'thickness *vs.* energy' dependence shown below) and (ii) results in a thinner crystal at high energies (low position of the red coloured band in the figures below).

The crystal thickness is determined as $d = (\Delta\theta/A)\cdot\sin(\theta+\alpha)$.

For the selected crystal thickness the length is given by $L = (\mathrm{XZ}\cdot\mathrm{Xapert.})/\sin(\theta+\alpha) + d/|\tan(\theta+\alpha)|$ and is calculated at the smallest Bragg angle.

Be 100 symmetric Bragg

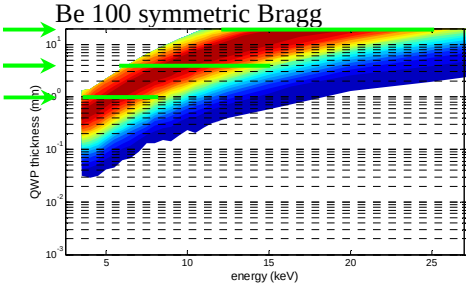

diamond 111 symmetric Bragg

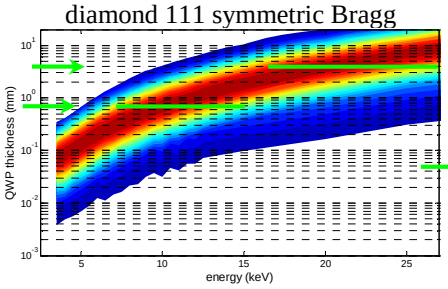

graphite 002 symmetric Bragg

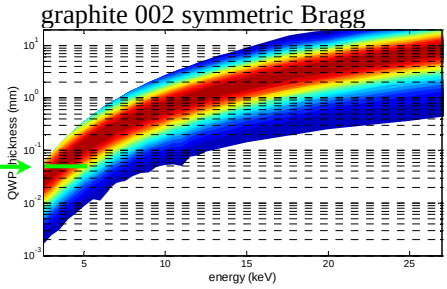

Be 010 asymmetric Laue, $\alpha = 60^{\circ}$

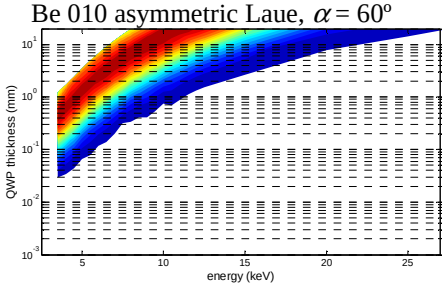

diamond 11–1 asym. Laue $\alpha = 70.5^{\circ}$

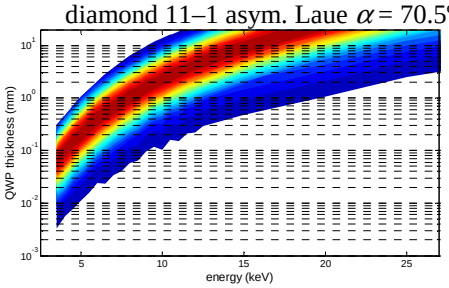

Be 010 asymmetric Laue, $\alpha = -60^{\circ}$

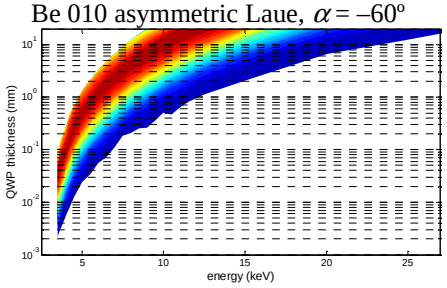

diamond 11–1 asym. Laue $\alpha = -70.5^{\circ}$

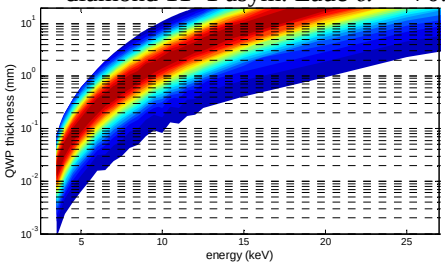

Be 002 symmetric Laue

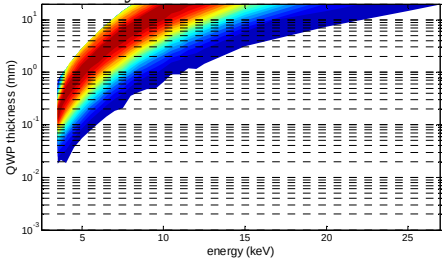

diamond 2–20 symmetric Laue

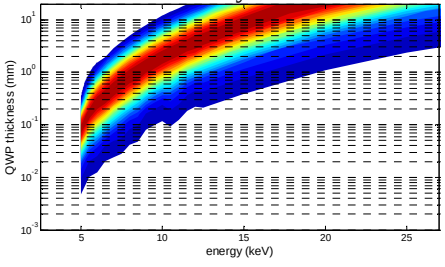

diamond 220 asym. Laue with $\alpha = 35.3^o$

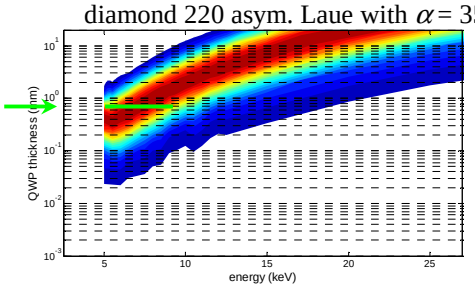

diamond 220 asym. Laue with $\alpha = -35.3^o$

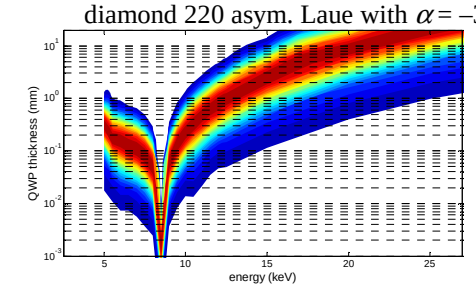

Summary:

The following crystals are selected (see the green horizontal lines in the above pictures):

Energy range	crystal		thickness (mm)	length (mm)
2.5–5 keV	graphite 002 sym Bragg		0.05	15
5–15 keV	opt. A	Be 100 sym Bragg (3.5–8 keV)	1	17
		Be 100 sym Bragg (7–15 keV)	4	39
	opt. B	diamond 220 asym Laue, $\alpha = 35.3^o$, (5–9 keV)	0.7	3
		diamond 111 sym Bragg (7–15 keV)		13
17–27 keV	opt. A	Be 100 sym Bragg	20	198
	opt. B	diamond 111 sym Bragg	4	51

The latter energy range requires big crystals which are hardly available for a reasonable price. It is recommended therefore to exclude this energy range from consideration.

The mosaicity of graphite is increased with its thickness. A usual good value for the mosaicity of bulk (2 mm) graphite layers is ~0.4°=1440 arcsec. Therefore this material is considered for the lowest energies only.

9 Performance of QWP

With the selected crystals used at specified energies and with the optimal apertures, the typical polarization rates are in the range 0.3–0.6. The polarization rate can be increased at the expense of intensity by closing the beam aperture.

The best achievable polarization rates for the selected crystals are shown below along with the transmission values. This time the crystal thickness is constant.

graphite 002 sym Bragg, 50 µm

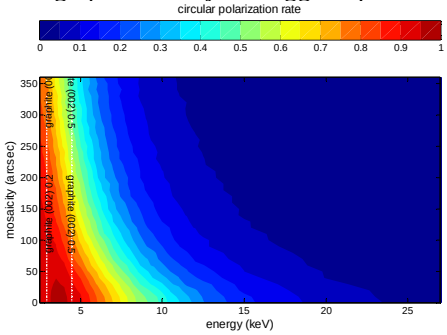

diamond 111 sym Bragg, 0.7 mm

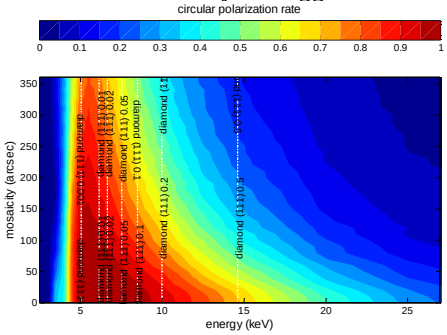

Be 100 sym Bragg, 4 mm

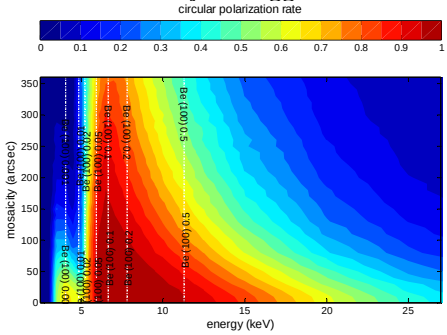

10 Performance of HWP

Two QWP crystals of the same type and thickness positioned one after the other in the x-ray beam transform horizontal linear polarization to vertical, thus forming an HWP. The vertically polarized x-rays, in combination with a crystal analyzer [1] can be used (i) for polarimetry [4] and (ii) and for momentum transfer dependent Raman studies. The latter application requires a good polarization rate.

The vertical linear polarization rate was calculated as

$$\tau = -\sin(2\psi)\,\mathrm{Re}\left\langle e^{i2\phi}\right\rangle, \qquad (6)$$

where the phase shift 2ϕ is due to two QWP crystals and the minus sign is introduced for the *vertical* polarization; the negative linear polarization rate values here mean the *horizontal* polarization.

The best achievable polarization rates for the selected crystals are shown below along with the transmission values. Notice the different polarization rate range: from –1 to 1.

graphite 002 sym Bragg, 2×50 µm | diamond 111 sym Bragg, 2×0.7 mm | Be 100 sym Bragg, 2×4 mm

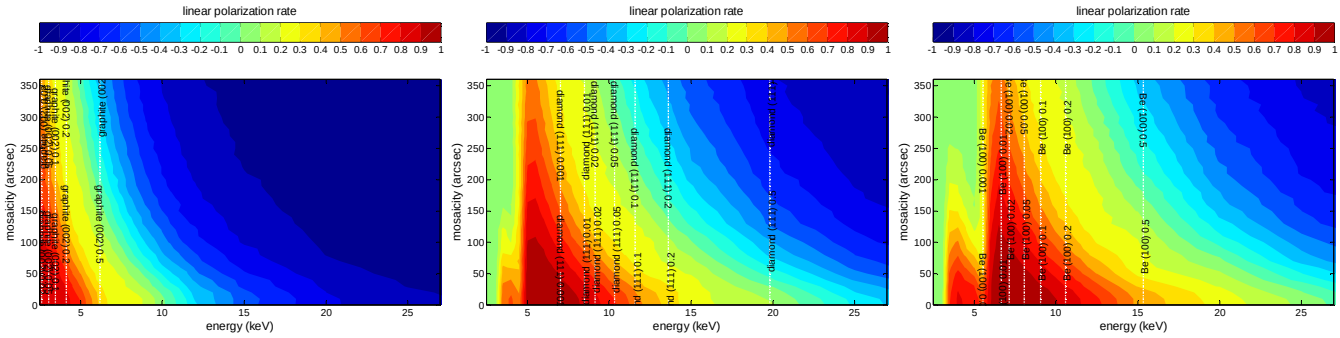

The polarization rates of HWP are lower than those of QWP. On one hand, this poses limitations to the usable energy range, and on the other hand, this means the presence of unpolarized background. It is expected that the HWP, in combination with the properly selected aperture, will serve as *depolarizer* in order to subtract the depolarized contribution from momentum transfer dependent Raman spectra.

11 3D models of spectrometer

Required are one goniometer with a moderate angular repeatability of ~1–10 arcsec and two linear translation stages to select the crystals and to insert/remove the second crystal set to be used for polarimetry or for $\pi/2$ rotation of the horizontal polarization plane.

low-energy case:

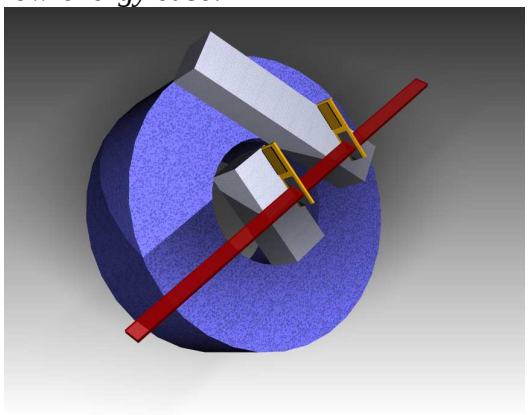

high-energy case:

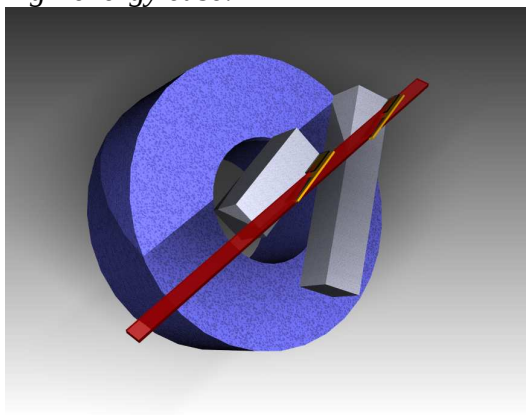

12 Conclusion

The optimal options for the crystal types and sizes have been determined. The final decision will be done basing on the available mosaicity values and prices of crystals.

References

[1] K. Klementiev, *Conceptual Design Report "X-ray emission spectrometer at the ALBA XAS beamline"* (2007) (see web page: http://www.cells.es/Beamlines/XAS/).

[2] K. Klementiev, *Conceptual Design Report "XAS beamline at the ALBA Synchrotron Light Facility"* (2006) (see web page: http://www.cells.es/Beamlines/XAS/).

[3] V. A. Belyakov and V. E. Dmitrienko, *Polarization phenomena in x-ray optics*, Uspekhi Fiz. Nauk. **158** (1989) 679–721, Sov. Phys. Usp. **32** (1989) 697–719

[4] C. Malgrange, *X-ray Polarization and Applications* in *X-ray and Neutron Dynamical Diffraction:Theory and Applications*, edited by A. Authier, S. Lagomarsino & B. K. Tanner, NATO ASI Ser., Ser. B: Physics **357** (1996) 91–109, Plenum Press: New York and London.

[5] M. Sanchez del Rio, R. J. Dejus, *XOP: A Multiplatform Graphical User Interface for Synchrotron Radiation Spectral and Optics Calculations*, SPIE Proc., 3152 (1997) 148; web page: http://www.esrf.fr/computing/scientific/xop2.1/.

[6] P. A. Lee, P. H. Citrin, P. Eisenberger and B. M. Kincaid, *Extended X-ray absorption fine structure - its strengths and limitations as a structural tool*, Rev. Mod. Phys. **53** (1981) 769–806.

[7] K. Klementiev, *Energy-dispersive Shadowrunner* (2007) based on Matlab script *Shadowrunner* by J. Juanhuix and J. Nicolás (2005).

[8] B. Lai and F. Cerrina, Nuc. Instrum. Methods A **246** (1986) 337.